# Investigation of the Structural and Electrical properties of Lanthanum and Samarium co-doped Ceria for Low Temperature Solid Oxide Fuel Cell Electrolytes Application

#### Lemessa Asefa Eressa

<sup>1</sup>Department of Physics, College of Natural & Computational Sciences, Ambo University, Ambo, Ethiopia.

Email: lemessaphys@gmail.com, lemessa.asefa@ambou.edu.et

#### **Abstract**

The aim of this study was to investigate the structural, morphological, and electrical properties of ceria co-doped with samarium and lanthanum (LSDC) for application as an electrolyte in solid oxide fuel cells operating at lower temperatures. To assess the crystal structure, microstructure, and electrical characteristics, techniques including X-ray diffraction (XRD), scanning electron microscopy (SEM), and impedance spectroscopy were employed. The findings from XRD indicated that all samples crystallized into a single-phase, cubic fluorite structure, with crystallite sizes ranging from 20 to 29 nm. Confirmation of grain formation, along with average grain sizes between 380 and 966 nm, as well as the presence of pores, was determined by the SEM micrograph. The conductivity values determined through impedance spectroscopy for the compositions  $Ce_{0.9}Sm_{0.05}La_{0.05}O_{1.95}$ ,  $Ce_{0.85}Sm_{0.05}La_{0.1}O_{1.925}$ ,  $Ce_{0.85}Sm_{0.1}La_{0.05}O_{1.925}$ , and  $Ce_{0.8}Sm_{0.1}La_{0.1}O_{1.9}$  were  $4.28\times10^{-3}$  S/cm,  $6.5\times10^{-3}$  S/cm,  $1.63\times10^{-2}$  S/cm, and  $1.13\times10^{-2}$  S/cm, respectively, at a temperature of 500°C in an air atmosphere. The activation energies calculated for the samples Ce<sub>0.9</sub>Sm<sub>0.05</sub>La<sub>0.05</sub>O<sub>1.95</sub>,  $Ce_{0.85}Sm_{0.05}La_{0.1}O_{1.925}$ ,  $Ce_{0.85}Sm_{0.1}La_{0.05}O_{1.925}$ , and  $Ce_{0.8}Sm_{0.1}La_{0.1}O_{1.9}$  were 0.83 eV, 0.76 eV, 0.64 eV, and 0.67 eV, respectively. Among the LSDC-series samples, the composition Ce<sub>0.85</sub>Sm<sub>0.1</sub>La<sub>0.05</sub>O<sub>1.925</sub> exhibited the highest ionic conductivities and the lowest activation energies across all measured temperatures. Additionally, every LSDC sample demonstrated ionic conductivities greater than 10<sup>-3</sup> S/cm, even at the reduced temperature of 400°C. These results collectively validated that the co-doping of samarium and lanthanum in ceria enhances its structure, morphology, and ionic conductivity, making it a viable strong electrolyte for applications in low-temperature solid oxide fuel cells.

Keywords: LT-SOFC; electrolyte; ceria; co-doping; electrical properties.

#### 1. Introduction

Solid oxide fuel cells (SOFCs) represent a promising electrochemical technology that converts chemical energy into electrical energy through simple redox reactions with minimum carbon emissions [1-9]. However, most SOFCs have been operated at very high temperatures (800-1000 °C), which in turn limits their applications [10]. Currently, the development of SOFCs focuses on reducing the operating temperature to medium temperatures (500-800°C) and low temperatures (300-500°C)[11]. As a result, the operating temperature was reduced to low temperatures (300-500°C) and medium temperatures around 500-800°C, leading to improved performance and subsequent commercialization of SOFCs as portable power sources[12]. However, lowering the operating temperature will result in a drop in the rate of electrocatalytic processes and an increase in electrolyte resistance [13]. Finding a different electrolyte with quick ion transport in the material is one way to overcome these difficulties[14]. Additionally, lowering the fuel cell's

operating temperature is becoming more and more crucial to extending the stability and lifespan of a SOFC. Additionally, expanding the range of electrolyte materials can lower the cost of cell production and material processing. Rare earth doped ceria-based materials have a better ionic conductivity at relatively lower temperatures and a lower activation energy than YSZ electrolyte[15]. Previously, the performance of single lanthanum doped ceria electrolyte was investigated for solid oxide fuel cell application in the intermediate temperature range (550-700°C) [16, 17]. However, literature results show that single-doped ceria-based oxides have limitations on their application as solid electrolytes due to their tendency to reduce. Ce<sup>4+</sup>(ionic conduction) to Ce<sup>3+</sup>(electronic conduction).

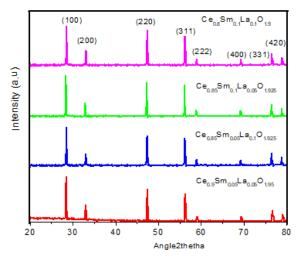


Figure 1.XRD patterns of LSDC- samples

Moreover, at low operating temperatures, grain boundary resistance is a significant inhibition to ionic conductivity [18]. Thus, research results showed that co-doping strategy is another option to improve the electrical properties of ceria based electrolytes at low temperature range by decreasing grain resistance and minimizing reduction of ceria[19, 20]. Therefore, the author aimed to have comprehensive investigation of structural, morphology and electrical properties of lanthanum and samarium co-doped ceria( $Ce_{1-x-y}Sm_xLa_yO_{2-\delta}$  (0.0  $\leq x = y \leq 0.05,0.1$ ) for use as an electrolyte for low temperature solid oxide fuel cell (LT-SOFC) applications.

#### 2. Experimental Methods

this study, cerium nitrate hexahydrate (Ce(NO<sub>3</sub>)<sub>3</sub>.6H<sub>2</sub>O)) 99.99% purity, Samarium nitrate 99.99% purity, hexahydrate  $((Sm(NO_3)_3.6H_2O))$ Lanthanum (III) nitrate hexahydrate ((La(NO<sub>3</sub>)<sub>3</sub>.6H<sub>2</sub>O)) 99.99% purity, Ammonium hydroxide (NH<sub>4</sub>OH), Citric acid (C<sub>6</sub>H<sub>8</sub>O<sub>7</sub>), Ethylene glycol ((CH<sub>3</sub>COOC<sub>2</sub>H<sub>5</sub>) were used as starting chemicals for the preparation of LSDC samples using sol-gel method. Initially, stoichiometric amounts of all nitrates were dissolved in distilled water under continuous stirring. Next, citric acid was added to the entire mixture of precursors in 1:1 molar ratio to take care of the entire molar ratio of metal to acid. So as to regulate the pH value to (pH to  $\approx$ 7), ammonium hydroxide was added drop by drop to the solution. Further, the entire mixture was stirred at 80°C for 3hours to make a homogenous solution. After 3hours, a viscous gel was formed which in turn placed in an oven to make an ash. Ash was calcined at 600°C for 2 hours to get rid of the carbonaceous materials. The resultant ash was ground continuously for 1hour in agate mortar to get a fine homogeneous powder. The powders were pressed with the help of a hydraulic press under a pressure of 200MPa into a circular pellet (8mm in diameter and 2 mm in thickness). Finally, the pellets were sintered in furnace at 1400°C for 2hours and prepared for impedance measurement.

#### 3. RESULT AND DISCUSSION

### 3.1 Structural Characterization by X-ray Diffract meter

The structural characterization of all the sintered LSDC samples were done at room temperature using Philips X-ray Diffractometer with  $Cuk_{\alpha}$  radiation ( $\lambda$ =1.54  $A^0$ ) operated at 40 kV and 30 mA in the 20 range of 20–80° with a step size of 0.02 and a time for step is 2s. Figure 1 illustrates the X-ray diffraction data of prepared samarium and lanthanum co-doped ceria samples. X-ray diffraction patterns of all the samples indexed to (hkl) parameters i.e. (111), (200), (220), (311), (222), (400), (331) and (420) indicating the formation of each composition with single phase cubic structure with JCPDS PDF: 34–0394 and space group Fm3m[21-23]. This confirms that no diffraction peaks resulting from impurity phases were observed in all LSDC samples, suggesting the formation of a homogeneous single polycrystalline phase.

The differences in ionic radius i.e. higher ionic radius of dopants compared to cerium lead to an increase in the lattice parameter values with increase in the dopant concentration, which is validated by the shift in powder X-ray diffraction(PXRD) patterns [24, 25]. The variation in the lattice parameter values with the composition were determined from the rietveld refinements of PXRD patterns. The crystallographic information i.e., crystal structure, lattice parameter and crystallite sizes of all the co-doped ceria samples were listed in Table 1.

Scherer equation is used to determine the crystallite size (D) from the PXRD data (i.e. (111) plane of reflection) of all the samples,

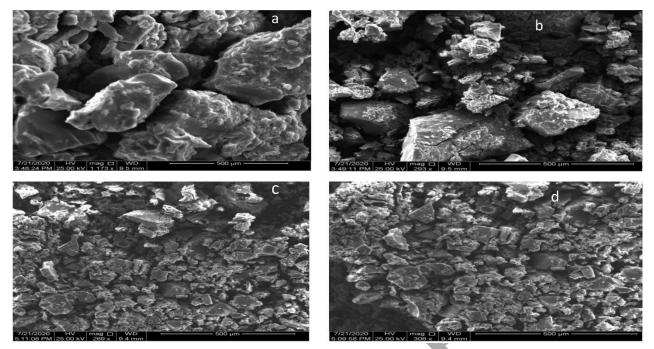
$$D = \frac{0.9\lambda}{\beta \cos \theta} \tag{1}$$

Where 'K' is the shape factor, ' $\lambda$ ' is the wavelength, ' $\theta$ ' is the diffraction angle and ' $\beta$ ' is the full

width half maxima. Table 1 describes the calculated crystallite sizes for each sample, which were all found to fall between 20 and 29 nm. This phenomenon suggests improvements in the crystallite size as a result of codoping strategy.

## **3.2.** Morphology Characterization by Scanning Electron Microscope

morphology of sintered  $Ce_{1-x-y}Sm_xLa_yO_{2-\delta}$  pellets was taken by fieldemission scanning electron microscope (FE-SEM, Carl Zeiss, EVO18). Figure 2 presents the SEM images of all the samples sintered at 1400°C for 2 hours with grains showing some pores. Calculations revealed that the average grain sizes of all the LSDC samples were in the range of 380 and 966 nm and indicated in Table 1. The ionic radius variation between the co-dopants samarium and lanthanum, as well as their concentrations, is what causes the diversity in grain size seen among samples. Additionally, it was produced as a result of their dissimilar morphologies, which led to uneven temperature treatments during sample synthesis.



 $Figure\ 2\ SEM\ graphs\ of\ (a)\ Ce_{0.9}Sm_{0.05}La_{0.05}O_{1.95}\quad (b)\ Ce_{0.85}Sm_{0.05}La_{0.1}O_{1.92\ 5}\quad (c)\ Ce_{0.85}Sm_{0.1}La_{0.05}O_{1.925}\ (d)\ Ce_{0.8}Sm_{0.1}La_{0.1}O_{1.925}$ 

Table 1 Crystallite size, grain size and lattice parameter of LSDC-samples

No.	Compositions	Crystallite Size (nm)	Grain Size (nm)	Lattice Parameter (Å)
1	$Ce_{0.9}Sm_{0.05}La_{0.05}O_{1.95}$	29	966	5.414
2	$Ce_{0.85}Sm_{0.05}La_{0.1}O_{1.925}$	26	840	5.416
3	$Ce_{0.85}Sm_{0.1}La_{0.05}O_{1.925}$	21	620	5.418
4	$Ce_{0.8}Sm_{0.1}La_{0.1}O_{1.9}$	20	380	5.417

Table 2. Resistances and conductivities of Ce<sub>0.9</sub>Sm<sub>0.05</sub> La<sub>0.05</sub>O<sub>1.95</sub> sample

Temperature( <sup>0</sup> C)	$Rg(\Omega)$	$Rgb(\Omega$	$R(\Omega$	$\sigma(S/cm)$
400	145.7	581.3	727	1.1x10 <sup>-3</sup>
450	117.38	227.81	345.19	$2.32x10^{-3}$
500	55.06	131.99	187.05	$4.28 \times 10^{-3}$

Table 3.Resistances and conductivities of  $e_{0.85}Sm_{0.05}La_{0.1}O_{1.925}$  sample

Temperature( <sup>0</sup> C)	$Rg(\Omega$	$Rgb(\Omega$	$R(\Omega$	$\sigma(S/cm)$
400	131.2	215.9	347.1	$2.3 \times 10^{-3}$
450	90.38	99.39	189.77	$4.2x10^{-3}$
500	42.27	81.6	123.87	$6.5 \times 10^{-3}$

Table 4. Resistances and conductivities of  $Ce_{0.85}Sm_{0.1}La_{0.05}O_{1.925}$  sample

Temperature( <sup>0</sup> C)	$Rg(\Omega$	$Rgb(\Omega$	$R(\Omega$	$\sigma(S/cm)$
400	28.5	52.3	80.8	9.9x10 <sup>-3</sup>
450	25.01	27.32	52.33	1.52x10 <sup>-2</sup>
500	22.54	26.56	49.1	1.63x10 <sup>-2</sup>

Table 5. Resistances and conductivities of  $Ce_{0.8}Sm_{0.1}\,La_{0.1}O_{1.9}$  sample

Temperature( <sup>0</sup> C)	$Rg(\Omega$	$Rgb(\Omega$	$R(\Omega$	$\sigma(S/cm)$
400	36.9	65.4	102.3	7.82x10 <sup>-3</sup>
450	34.00	45.12	79.12	1.01x10 <sup>-2</sup>
500	30.02	40.39	70.39	1.13x10 <sup>-2</sup>

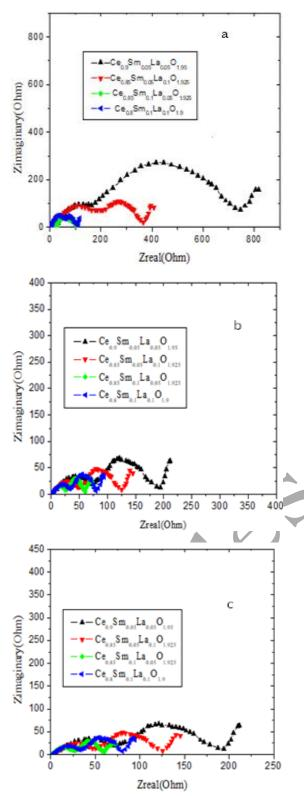


Figure 3 Nyquist Plots of LSDC-Samples at Temperatures of a)  $400^{\circ}$ C b)  $450^{\circ}$ C and c) $500^{\circ}$ C.

#### 3.3. Electrical analysis

AC impedance measurements were carried out on pellets coated with silver paint on both surfaces employing Auto lab impedance Analyser in the frequency range 1Hz-1MHz and from room temperature to 500°C. The impedance spectra consist of graphs with real part Z' on

X-axis and negative imaginary part Z" on Y-axis known as complex impedance spectra and is a materials characteristic conducting nature [26-28]. In many cases, complex impedance spectra characterized by three successive semi-circle contributions; lower frequency semi-circle is corresponds to electrode contribution, medium frequency semi-circle corresponds to grain boundary contribution and the higher frequency semi-circle corresponds to grain contribution[29, 30] The complex impedance analysis of lanthanum and samarium co-doped ceria samples was carried out in the temperature range from 400 to 500°C.

Figure 3 (a), (b) and (c) represents the complex impedance plots at 400°C, 450°C and 500°C respectively for codoped ceria samples with a combination of three semicircles correspond to grain, grain-boundary and electrode contributions. As it can be observed form Figure 3 (a), (b) and (c), the curves seem to be clear semicircles. With the increase in the concentration and temperature, the semicircles were decreased gradually in size. The clear semicircles were observed only when homogeneous grain size distribution and grain shapes present in the co-doped ceria ceramics. As the temperature increases, the area under the semi-circle decreases. This resulted in the decrease of the impedance which in turn leads to an increase in the conductivity. The area under the semicircles also decreased with increase in the temperature and the area under the semi-circle found to be the least for the composition Ce<sub>0.85</sub>Sm<sub>0.1</sub>La<sub>0.05</sub>O<sub>1.925</sub>.at all temperatures among LSDC samples. This indicates, the decrease in the impedance of the samples leads to an increase in the conductivity. At higher temperature, the complex impedance plots not show any arc at the lower frequency region and this observation recommends virtually that there is no contribution of electrode process to the electrical conductivity [26, 31, 32].

The total resistance (sum of grain and grain-boundary resistance i.e.  $R_T = Rg + Rgb$ ) of all the samples, at all temperatures were calculated from the intercepts of semicircle on the real impedance axis [32-34]. The total resistance is given by

$$R_T = R_g + R_{gb} \tag{2}$$

Where Rg and Rgb stand for the resistance of grain interior and grain boundary respectively.

Then, the ionic conductivity ( $\sigma$ ) of each sample was calculated using the equation:

$$\sigma = \frac{l}{RA} \tag{3}$$

where l is the thickness of sample and A is the cross-sectional area. Through curve fitting a circle to the semi circles on the impedance spectra, the sample total resistance(R) was obtained using Equation (2). Then, the conductivity values of samples were calculated from the resistance values using Equation (3). This result presented in Tables 2, 3, 4 and 5 below.

As indicated in Tables 2, 3, 4 & 5, the conductivity of compositions  $Ce_{0.9}Sm_{0.05}La_{0.05}O_{1.95}, \\ Ce_{0.85}Sm_{0.05}La_{0.1}O_{1.925} \quad , \quad Ce_{0.85}Sm_{0.1}La_{0.05}O_{1.925} \quad \text{and} \\ Ce_{0.8}Sm_{0.1}La_{0.1}O_{1.9} \text{ obtained were } 4.28x10^{-3}\text{S/cm, } 6.5x10^{-3}\text{S/cm, } 1.63x10^{-2}\text{S/cm} \text{ and } 1.13x10^{-2}\text{S/cm} \text{ respectively at } 500^{0}\text{C} \text{ in air atmosphere.}$ 

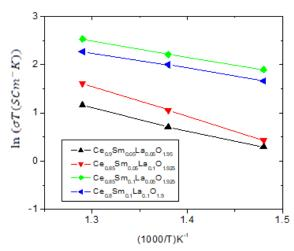


Figure 4 Arrhenius plots for total conductivity of LSDC-samples

Table 6. Activation energy of LSDC- samples

No	Sample	Ea(eV)
1	$Ce_{0.9}Sm_{0.05}La_{0.05}O_{1.95}$	0.83
2	$Ce_{0.85}Sm_{0.05}La_{0.1}O_{1.925}$	0.76
3	$Ce_{0.85}Sm_{0.1}La_{0.05}O_{1.925}$	0.64
3	$Ce_{0.8}Sm_{0.1}La_{0.1}O_{1.9}$	0.67

Generally, the higher dopant concentration, the higher concentration of mobile ion (ion oxide vacancy) that leads to the higher ionic conductivity. For co-doped ceria with the ratio of Sm<sup>3+</sup> (r = 1.08A<sup>0</sup>) dopant and La<sup>3+</sup> (r = 1.16A<sup>0</sup>) dopant was 1:1. The conductivity of Ce<sub>0.8</sub>Sm<sub>0.1</sub>La<sub>0.1</sub> O<sub>1.9</sub> was higher than Ce<sub>0.9</sub>Sm<sub>0.05</sub>La <sub>0.05</sub> O<sub>1.95</sub>. This happens due to the greater lattice parameter of Ce<sub>0.8</sub>Sm<sub>0.1</sub>La<sub>0.1</sub> O<sub>k9</sub> (5.417 Å) which in turn facilitates fast diffusion of oxygen ions contributing greater ionic conductivity than in Ce<sub>0.8</sub>Sm<sub>0.1</sub>La<sub>0.1</sub> O<sub>1.9</sub> which has smaller lattice parameter of 5.414 Å. On the other hand, for co-doped ceria with total dopants concentration of 15% or the ratio between Sm<sup>3+</sup> dopant and La<sup>3+</sup> was 1:2 or 2:1, the conductivity of Ce<sub>0.85</sub>Sm<sub>0.1</sub>La<sub>0.05</sub>O<sub>1.925</sub> is greater than conductivity of Ce<sub>0.85</sub>Sm<sub>0.05</sub>La<sub>0.1</sub>O<sub>1.925</sub>. That means, further increasing of the lanthanum concentration leads to the formation of ion clusters which results in the deep traps to oxygen vacancies results in lowering the concentration of oxygen vacancies ultimately decrease the ionic conductivity of the sample. This is created as a result of big difference ionic radii of La3+ (1.16 Å) than between the Ce<sup>4+</sup>(0.970Å) which is consistent with literature reports[23]. But, increasing concentration of Sm3+ into ceria increases the total conductivity. That means, the ionic conductivity of Ce<sub>0.85</sub>Sm<sub>0.1</sub>La<sub>0.05</sub> O<sub>1.925</sub> was higher than Ce<sub>0.85</sub>Sm<sub>0.05</sub>La <sub>0.1</sub>O<sub>1.925</sub>. This due to the ionic radii of Sm<sup>3+</sup> which is more close to the critical ionic radii (1.038A<sup>0</sup>) than ionic radii of lanthanum[35]. property enhances the mobility of oxygen vacancies contributing highest ionic conductivity  $Ce_{0.85}Sm_{0.1}La_{0.05} \ O_{1.925}$  than in  $Ce_{0.85}Sm_{0.05}La_{0.1}O_{1.925}$ sample.

The temperature dependence of ionic conductivity often follows an Arrhenius relation:

follows an Arrhenius relation:  

$$\sigma T = \sigma_o e^{-Ea/\kappa T}$$
where  $Ea$  is the activation energy for conduction,  $T$  is the

temperature, k is the Boltzmann's constant and  $\sigma_o$  is a preexponential factor. The total ionic conductivities of LSDC- samples sintered at  $1400^{\circ}$ C for 2hours was presented in Figure 4 in the form of  $\ln(\sigma T)$  versus  $(10^3/T)$ . The value of Ea and  $\sigma_o$  were found from the slope and intercept of the graph respectively.

The Arrhenius plot described in Figure 4 reveals that the conductivity of all the LSDC-samples increased exponentially with temperature. This was possibly because of thermal excitation which enhances the kinetic energy of carriers and force oxygen ions to pass through oxygen vacancies in a higher speed. As the temperature rises, there exists stronger diffusion ability of oxygen ions, which ultimately lead to the enhancement of conductivity.

As it can be observed from Figure 4, the graph of  $Ce_{0.85}Sm_{0.1}La_{0.05}O_{1.925}$  lies above the graphs of other LSDC-samples. This shows that the conductivity of  $Ce_{0.85}Sm_{0.1}La_{0.05}O_{1.925}$  sample is the highest of all the other LSDC-samples. This could be due to formation of more number of oxygen vacancies and suppression of ordering of oxygen vacancies in  $Ce_{0.85}Sm_{0.1}La_{0.05}O_{1.925}$  than in other LSDC-samples. This phenomena leads to a decrease in the activation energy for diffusion of  $O^{2-}$  ions in  $Ce_{0.85}Sm_{0.1}L_{0.05}O_{1.925}$  sample.

Double doping lanthanum and samarium in ceria increases the oxygen vacancy disorder which helps to improve the grain conductivity. The increase of lattice constant caused by optimum lanthanum doping enlarges the channel of oxygen ion transport which also improves the grain conductivity. However, lattice distortion may occur with further increase in lanthanum content due to the big difference between the ionic radii of  $La^{3+}$  (1.16 Å) than  $Ce^{4+}(0.970\text{Å})$  as reported in previous literature [36]. Table 6 shows that the activation energy of LSDCsamples obtained by fitting of the data in Figure 3 to Arrhenius relations Equation (4). In this study, the calculated activation energies of samples  $Ce_{0.9}Sm_{0.05}La_{0.05}O_{1.95}$  $Ce_{0.85}Sm_{0.05}La_{0.1}O_{1.925}$ ,  $Ce_{0.85}Sm_{0.1}La_{0.05}O_{1.925}$  and  $Ce_{0.8}Sm_{0.1}La_{0.1}O_{1.9}$ 0.83eV, 0.76eV, 0.64eV and 0.67eV respectively. The activation energy of Ce<sub>0.85</sub>Sm<sub>0.1</sub>La<sub>0.05</sub>O<sub>1.925</sub> has the least activation energy which results with the greatest diffusion of oxygen ions (greatest ionic conductivity) in the sample than other LSDC sample series at all measurements.

In general, the addition of trivalent elements (La<sup>3+</sup> and Sm<sup>3+</sup>) to the structure of pure ceria often resulted in an increase in the value of the crystal lattice parameter of LSDC- samples. As a result, the unit cell expands and oxygen vacancies are created, which are necessary for the conduction process. This facilitates the movement of oxygen ions and reduces the resistances of the grains and grain boundaries. All these factors ultimately resulted in an increase in the ionic conductivity and lowering of activation energy of the LSDC-samples. Hence, codoping strategy is a good method in improving the structural and electrical properties of LSDC- samples at low temperature. This may be due to increase in the effective ionic radii of co-dopants which is close to the critical ionic radii (1.038 Å) for doped ceria [28]. As the ionic radii of these dopant cations are closer to the critical

ionic radii of host, the lower activation energy effect to the diffusion of oxygen vacancies resulted in to the greater the conductivity of the electrolyte.

Based on electrical analysis described on tables 4 & 6, the formation of high concentrated oxygen vacancies of Ce<sub>0.85</sub>Sm<sub>0.1</sub>La<sub>0.05</sub>O<sub>1.925</sub> resulted in the highest total ionic conductivity of 1.63x10<sup>-2</sup>S cm<sup>-1</sup>with minimum activation energy of 0.64eV. In general, the conductivity of codoped LSDC- samples obtained in the temperature range 400-500<sup>0</sup>C in this work was higher than that of single lanthanum doped ceria previously reported[37, 38].

#### 4. Conclusions

The advance of SOFC in lowering its operating temperature has targeted the use of electrolytes which operates at lower temperatures. In order to attain this goal, co-doping strategy was employed to samarium and lanthanum co-doped ceria electrolytes prepared through sol-gel synthesis method. The XRD result reveals that all the samples were single phase with cubic fluorite-type structure. The SEM micrograph definitely showed the presence of grains with presence of pores. The impedance spectroscopy measurements indicated that all the samples showed conductivities higher than 10<sup>-3</sup>Scm<sup>-1</sup> at low temperature range (400-500°C). All of these results support the notion that samarium and lanthanum codoping of ceria improved its structural and electrical properties. The findings confirmed that co-doped ceria with samarium and lanthanum is a promising electrolyte for solid oxide fuel cell at low temperature. For better work and comprehensive investigation of these material properties, performing mechanical strength tests, EDS measurements, Raman measurements, BET measurements and use of advanced impedance spectroscopy (which measures frequency up to 40MHz) were some of the recommendations made as a future work.

#### **Data Availability Statement**

The data that support the findings of the study are available within the article.

#### **Conflicts of Interest**

The author declares no conflicts of interest

#### **Funding**

No funding was received for this research

#### Acknowledgments

I am gratefully acknowledged the Addis Ababa Science and Technology University (AASTU) for their support during this work.

#### References

- 1. Changan, T., et al., *Preparation and characterization of Ce0. 8La0. 2–xYxO1. 9 as electrolyte for solid oxide fuel cells.* Journal of Rare Earths, 2014. **32**(12): p. 1162-1169.
- 2. Wang, F.-Y., et al., Study on Gd and Mg co-doped ceria electrolyte for intermediate temperature solid oxide fuel cells. Catalysis Today, 2004. 97(2-3): p. 189-194.
- 3. Jaiswal, N., et al., Ceria co-doped with calcium (Ca) and strontium (Sr): a potential candidate as a solid electrolyte for intermediate temperature solid oxide fuel cells. Ionics, 2014. 20: p. 45-54.
- 4. Singhal, S.C. and K. Kendall, *High-temperature solid oxide fuel cells: fundamentals, design and applications.* 2003: Elsevier.
- 5. Mat, M.D., et al., *Development of cathodes for methanol and ethanol fuelled low temperature (300–600° C) solid oxide fuel cells.* International journal of hydrogen energy, 2007. **32**(7): p. 796-801.
- 6. Park, S., J.M. Vohs, and R.J. Gorte, *Direct oxidation of hydrocarbons in a solid-oxide fuel cell*. Nature, 2000. **404**(6775): p. 265-267.
- 7. Sındıraç, C., A. Büyükaksoy, and S. Akkurt, *Electrical properties of gadolinia doped ceria electrolytes fabricated by infiltration aided sintering*. Solid State Ionics, 2019. **340**: p. 115020.
- 8. Costilla-Aguilar, S., et al., *Gadolinium doped ceria nanostructured oxide for intermediate temperature solid oxide fuel cells.* Journal of Alloys and Compounds, 2021. **878**: p. 160444.
- 9. Choudhury, A., H. Chandra, and A. Arora, *Application of solid oxide fuel cell technology for power generation—A review*. Renewable and Sustainable Energy Reviews, 2013. **20**: p. 430-442.
- 10. Arabaci, A., *Ceria-based solid electrolytes for IT-SOFC applications*. ACTA PHYSICA POLONICA A, 2020. **137**: p. 530-534.
- 11.Xia, Y., et al., *Electrical properties optimization of calcium Co-doping system: CeO2–Sm2O3*. International journal of hydrogen energy, 2012. **37**(16): p. 11934-11940.
- 12. Omar, S., E.D. Wachsman, and J.C. Nino, *Higher ionic conductive ceria-based electrolytes for solid oxide fuel cells*. Applied Physics Letters, 2007. **91**(14).

- 13. Hardian, A. Synthesis and characterization of Gd and Er co-doped ceria as solid electrolyte for IT-SOFC via solid state method. in 2011 2nd International Conference on Instrumentation, Communications, Information Technology, and Biomedical Engineering. 2011. IEEE.
- 14. Fan, L., et al., *Nanomaterials and technologies for low temperature solid oxide fuel cells: recent advances, challenges and opportunities.* Nano Energy, 2018. **45**: p. 148-176.
- 15. Shajahan, I., et al., *Praseodymium doped ceria as electrolyte material for IT-SOFC applications*. Materials Chemistry and Physics, 2018. **216**: p. 136-142.
- 16. Singh, K., R. Kumar, and A. Chowdhury, *Lanthanum doped Ceria nanoparticles: A promising material for energy applications*. Materials Today: Proceedings, 2018. **5**(11): p. 22993-22997.
- 17. Sumi, H., et al., Lanthanum-doped ceria interlayer between electrolyte and cathode for solid oxide fuel cells. Journal of Asian Ceramic Societies, 2021. 9(2): p. 609-616.
- 18. Singh, N.K., et al., *Electrical conductivity of undoped, singly doped, and co-doped ceria.* Ionics, 2012. **18**: p. 127-134.
- 19. Zając, W. and J. Molenda, *Electrical conductivity of doubly doped ceria*. Solid State Ionics, 2008. **179**(1-6): p. 154-158.
- 20.Li, B., et al., *Electrical properties of ceria Co-doped with Sm3+ and Nd3+*. Journal of Power Sources, 2010. **195**(4): p. 969-976.
- 21. Accardo, G., et al., *Improved microstructure and sintering temperature of bismuth nano-doped GDC powders synthesized by direct sol-gel combustion*. Ceramics International, 2018. **44**(4): p. 3800-3809.
- 22. Kahlaoui, M., et al., Synthesis and electrical properties of co-doping with La3+, Nd3+, Y3+, and Eu3+ citric acid-nitrate prepared samarium-doped ceria ceramics. Ceramics International, 2013. **39**(4): p. 3873-3879.
- 23. Venkataramana, K., et al., *Investigation on La3+ and Dy3+ co-doped ceria ceramics with an optimized average atomic number of dopants for electrolytes in IT-SOFCs.* Ceramics International, 2018. **44**(6): p. 6300-6310.
- 24. Venkataramana, K., et al., *Structural, electrical and thermal expansion studies of tri-doped ceria electrolyte materials for IT-SOFCs.* Journal of Alloys and Compounds, 2017. **719**: p. 97-107.
- 25. Shannon, R.D., Revised effective ionic radii and systematic studies of interatomic distances in halides and chalcogenides. Acta crystallographica section A: crystal physics, diffraction, theoretical and general crystallography, 1976. **32**(5): p. 751-767.
- 26.Ramesh, S. and K.J. Raju, *Preparation and characterization of Ce1-x (Gd0. 5Pr0. 5) xO2 electrolyte for IT-SOFCs.* international journal of hydrogen energy, 2012. **37**(13): p. 10311-10317.
- 27. Anjaneya, K., et al., *Preparation and characterization of Ce1-xGdxO2-\delta (x=0.1–0.3) as solid electrolyte for intermediate temperature SOFC.* Journal of alloys and compounds, 2013. **578**: p. 53-59.
- 28.Kumar, V.P., et al., *Thermal and electrical properties of rare-earth co-doped ceria ceramics*. Materials Chemistry and Physics, 2008. **112**(2): p. 711-718.
- 29. Arabaci, A., Effect of Sm and Gd dopants on structural characteristics and ionic conductivity of ceria. Ceramics International, 2015. **41**(4): p. 5836-5842.
- 30.Badwal, S., F. Ciacchi, and D. Milosevic, *Scandia–zirconia electrolytes for intermediate temperature solid oxide fuel cell operation.* Solid State Ionics, 2000. **136**: p. 91-99.
- 31. Kumar, K.N., et al., *Dielectric features, relaxation dynamics and ac conductivity studies on Ag+ mixed lead arsenate glass ceramics*. Journal of Materials Science: Materials in Electronics, 2018. **29**(2): p. 1153-1172.
- 32. Wu, Y.-C. and C.-C. Lin, *The microstructures and property analysis of aliovalent cations (Sm3+, Mg2+, Ca2+, Sr2+, Ba2+) co-doped ceria-base electrolytes after an aging treatment.* International journal of hydrogen energy, 2014. **39**(15): p. 7988-8001.
- 33. Hauch, A., M. Mogensen, and A. Hagen, *Ni/YSZ electrode degradation studied by impedance spectroscopy—Effect of p (H2O)*. Solid State Ionics, 2011. **192**(1): p. 547-551.
- 34.Hu, Q., et al., *The preparation and electrical properties of La doped Er0. 2Ce0. 801. 9 based solid electrolyte.* International journal of Electrochemical Science., 2017. **12**(8): p. 7411-7425.

- 35.Omar, S., et al., *Crystal structure–ionic conductivity relationships in doped ceria systems*. Journal of the American Ceramic Society, 2009. **92**(11): p. 2674-2681.
- 36. Haile, S.M., Fuel cell materials and components. Acta materialia, 2003. 51(19): p. 5981-6000.
- 37. Mori, T., et al., *Electrolytic Properties and Nanostructural Features in the La2 O 3 CeO2 System.* Journal of the Electrochemical Society, 2003. **150**(6): p. A665.
- 38. Stojmenović, M., et al., *Structural, morphological, and electrical properties of doped ceria as a solid electrolyte for intermediate-temperature solid oxide fuel cells.* Journal of Materials Science, 2015. **50**: p. 3781-3794.

